The Kinematics of CMEs using Multiscale Methods

Jason P. Byrne[1], Peter T. Gallagher[1], R. T. James McAteer[1], C. Alex Young[2]

[1] Astrophysics Research Group, School of Physics, Trinity College Dublin, Dublin 2, Ireland

[2] ADNET Systems Inc., NASA Goddard Space Flight Center, Greenbelt, MD 20771, USA

email: jbyrne6 @ tcd.ie

1. Abstract

The kinematics of CMEs are derived through multiscale methods. The transient nature of CMEs means traditional image analysis can be difficult to interpret, so we exploit the scale dependence inherent in CME data with a multiscale decomposition (akin to a Canny edge detector). These methods are applied in a non-subjective manner and are computationally efficient at extracting faint or noisy CMEs from large volumes of data. A spatiotemporal filter highlights the CME front as it propagates in time, allowing characterisation through an ellipse fitting routine. It is then possible to extract the kinematics (height, velocity, acceleration) and changing morphology (width, orientation) in order to compare with the predictions of theory. The height-time curves of some CMEs have been shown to differ from the CACTus and CDAW catalogues. Although the resulting kinematic curves are fit with the constant acceleration model, within the derived error bounds certain events could also be fit by a non-constant acceleration model. This implies a more dynamic CME propagation than previous studies have indicated.

2. Background & Motivation

Several theoretical models have been proposed to describe CMEs.
In the ***flux-rope model***[1] foot-point motions trigger the eruption; the acceleration is then determined by the flux-rope geometry.
The ***breakout model***[2] is based on magnetic reconnection between overlying field lines and neighbouring flux systems.
Observational studies of CME data are necessary to test such models.

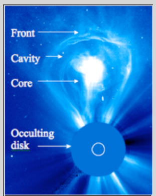

Fig.1: *A canonical CME.*

The diffuse nature of CMEs means their detection with traditional imaging techniques is difficult. Thus advanced image processing methods are necessary to:

1) Highlight and extract CMEs in coronagraph images,
2) Accurately measure the morphological and kinematical properties of observations[3],
3) Compare these results with theoretical models.

3. Multiscale Edge Detection

We explore a method of multiscale decomposition on an image through the use of ***low and high pass filters***; using a Gaussian θ and a derivative-of-Gaussian ψ respectively[4]. Since θ is separable in x and y we can write:

$$\psi_x(x,y) = \frac{\partial\theta(x)}{\partial x}\theta(y), \qquad \psi_y(x,y) = \theta(x)\frac{\partial\theta(y)}{\partial y}$$

Successive convolutions of an image with the filters produces different scales of decomposition, with the high-pass filtering providing the wavelet transform of the image in each direction (the rows and columns in the top panels of Fig. 2):

$$W_x I = \psi_x(x,y) * I(x,y), \qquad W_y I = \psi_y(x,y) * I(x,y)$$

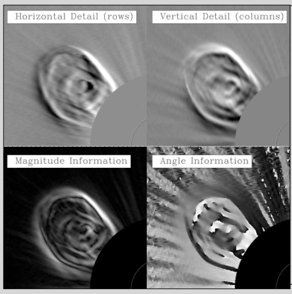

Fig.2: *The top panels show the horizontal and vertical detail from the high pass filtering of a CME observed by LASCO/C2 on the 1 Apr. 2004. The bottom panels indicate the magnitude (edge strength) and angle information (in the range 0-360°) from the resulting gradient space. Here scale 5 of the wavelet decomposition was chosen for its high signal-to-noise ratio. The CME is very efficiently highlighted at this scale.*

Akin to a Canny edge detector[5], these horizontal and vertical wavelet coefficients are combined to form the gradient space for each scale:

$$\Gamma(x,y) = [W_x I, \quad W_y I]$$

where the gradient information has an angular component α and magnitude (edge strength) M, illustrated in bottom of Fig. 2:

$$\alpha(x,y) = \tan^{-1}\left(W_x I / W_y I\right)$$

$$M(x,y) = \sqrt{(W_x I)^2 + (W_y I)^2}$$

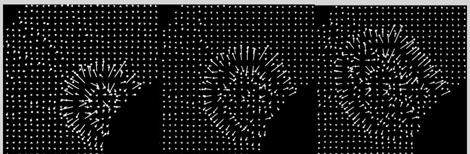

Fig.3: *The vectors plotted represent the combined magnitude and angle information determined from the gradient space showing the CME propagation very effectively.*

Plotting an overlay of arrows, whose magnitude and angle represent the gradient, highlights the CME as it propagates. Implementing a ***spatiotemporal filter*** extracts the motion of the CME, neglecting streamers and noise (see Fig. 3). This method of CME localisation:

1) overcomes the subjectivity of a user-specific bias,
2) negates the need for differencing thus minimising errors,
3) can be extended for use in automated CME detections.

Non-Maxima Suppression

The gradient information is further used in a ***pixel chaining*** algorithm[6]. This suppresses non-maxima pixel values and connects a line along edges, essentially defining the CME front (Fig. 4).

Characterisation: Ellipse Fitting

An ellipse fit provides the kinematics and morphology of the expanding CME structure (Fig. 4). Kinematical analysis includes height, velocity and acceleration. Changing morphology of the ellipse provides the angular width, inclination angle, and radius of curvature.

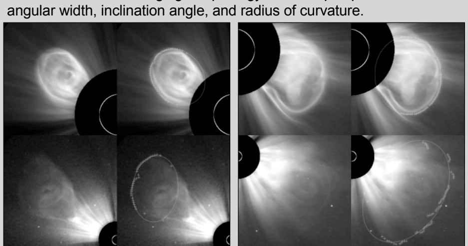

Fig.4: *The C2 and C3 images for the 1 Apr. 2004 CME (left) and the 2 Jan. 2000 CME (right). Also shown are the points along the corresponding CME fronts detected with multiscale analysis, and the resulting ellipse fit to these points.*

4. CME Kinematics & Morphology

2 January 2000

From Fig. 5, below, we conclude:

1) The height-time plot has a trend not unlike CDAW[7] however the offset of certain points may be an artifact of how the running differences are scaled for display or subjectively interpreted.

2) The velocity fit is not satisfied by a linear model. The velocity points range from 200-800 km s^{-1}. CDAW quotes a single velocity of 603 km s^{-1} while CACTus[8] quotes 512 km s^{-1}.

3) The acceleration profile indicates an early decreasing phase from 100 m s^{-2} down to zero. if not decelerating further. ***This event implies the constant acceleration model is not sufficient***.

1 April 2004

From Fig. 6, below, we conclude:

1) The height-time plot again has a trend similar to CDAW however the offset of certain points is still apparent, notably in the C3 field of view above 6 solar radii.

2) The velocity fit is almost satisfied by a linear model ranging from 350-500 km s^{-1}. CDAW quotes a single velocity of 460 km s^{-1} while CACTus quotes 487 km s^{-1}.

3) The acceleration profile is fit with the constant acceleration model, however there may be a slight indication of an early decreasing acceleration phase from 100 m s^{-2} down to zero (within errors this is not certain). The model gives a constant acceleration of approx. 6 m s^{-2}.

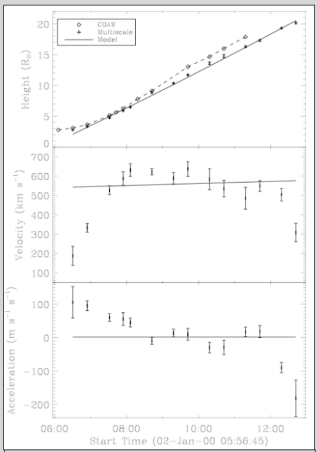

Fig.5: *The kinematics of the 2 Jan. 2000 CME. The model is a second order fit to the data:* $h_0+v_0t+a_0t^2/2$

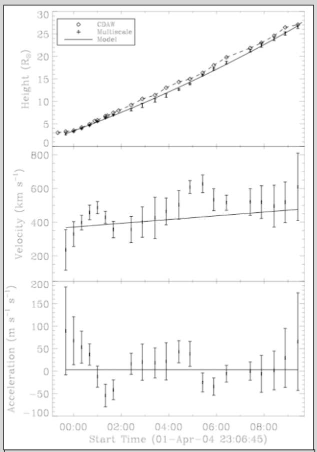

Fig.6: *The kinematics of the 1 Apr. 2004 CME. The model is a second order fit to the data:* $h_0+v_0t+a_0t^2/2$

CME Expansion

The ellipse fit gives an indication of the morphology of CMEs, and the ***angular width*** of these two events is discussed here.

The analysis of the 2 Jan. 2000 CME indicated a high early acceleration leading to a non-linear increasing velocity. From Fig. 7, below, it is seen that this event had a large expansion from approx. 50-100°.

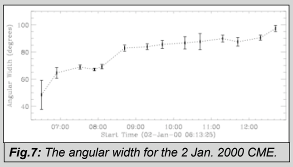

Fig.7: *The angular width for the 2 Jan. 2000 CME.*

The analysis of the 1 Apr. 2004 CME indicated that, within errors, the constant acceleration model was approx. 6 m s^{-2}. From Fig. 8, below, the angular width is almost constant, varying from 45-35°.

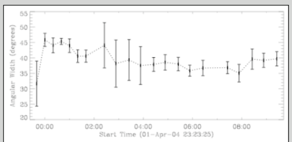

Fig.8: *The angular width for the 1 Apr. 2004 CME.*

There is thus a ***possible link between the CME angular width and speed***, where the above high-acceleration event of 2 Jan. 2000 showed a super-radial expansion, and the low-acceleration of 1 Apr. 2004 was radially expanding.

It may therefore be suggested that the ***non-radial expansion is indicative of highly dynamic cases where the constant acceleration model may not be sufficient.***

5. Future Directions

This work is an initial indication that the constant acceleration model may not always be accurate. Further ***studies on more events*** are necessary.

These methods will be applied to ***STEREO data***, whereby the combined view-points can provide further kinematic constraints, or lead to 3D reconstructions.

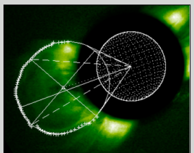

Fig.9: *Multiscale analysis and characterisation of the 25 Jan. 2007 CME observed by COR1.*

Our methods have been designed with ***automated detections and characterisations*** in mind. This is necessary for today's large data volume and for space weather forecasting.

Multiscale analysis can be explored further; there are many ***other multiscale transforms*** that may increase accuracy in CME detections (e.g. anisotropic wavelets and curvelets).

6. References

1. Krall, J., Chen, J., & Santoro, R., 2000, ApJ, 539, 964
2. Antiochos, S. K., DeVore, C. R. & Klimchuk, J. A., 1999, ApJ, 510, 485
3. Gallagher, P. T., Lawrence, G. R. & Dennis, B. R., 2003, ApJ, 588, L53
4. Starck, J. L. and Murtagh, F., Astronomical Image and Data Analysis, Springer, 2002
5. Young, C. A. & Gallagher, P. T., 2008, Sol. Phys., *submitted*
6. McAteer, R. T. J., Young, C. A., Ireland, J., Gallagher, P. T., Byrne, J. P. 2008, Sol. Phys., *submitted*
7. Yashiro, S., Gopalswamy, N., Michalek, G., St. Cyr, O. C., Plunkett, S. P., Rich, N. B. & Howard, R. A., 2005, ApJ, 619, 599
8. Robbrecht, E. & Berghmans, D., 2004, A&A, 425, 1097

JPB is grateful to the NASA/LWS program, and is supported by Science Foundation Ireland's Research Frontiers Programme. JMA is grateful to the STEREO/COR1 team and is on a Marie Curie Fellowship.